ISCI, Volume *22*

Supplemental Information

High-Throughput Platform for Optoacoustic Probing of Genetically Encoded Calcium Ion Indicators

Urs A.T. Hofmann, Arne Fabritius, Johannes Rebling, Héctor Estrada, X. Luís Deán-Ben, Oliver Griesbeck, and Daniel Razansky

1 Transparent Methods

1.1 Optoacoustic microscope

Pulsed Optoacoustic (OA) excitation was achieved by a wavelength tunable dye laser (Credo, Sirah Lasertechnik, Germany) which was pumped by a 532 nm Nd:YAG laser (IS811-E, Edgewave, Germany) at up to 10 kHz. The use of Pyrromethene 597 (Sirah Lasertechnik, Germany) allowed wavelength tuning over a range of 558 nm to 587 nm, while alternative dyes enable excitation in the entire visible and NIR range. The dye laser was tuned to an output wavelength of 560 nm (0.15 nm bandwidth) corresponding to the peak absorption wavelength of R-GECO1 (Shen et al. 2018). A broadband $\lambda/2$-waveplate (AHWP10M-600, Thorlabs, USA) in combination with a polarizing beam splitter (PBS251, Thorlabs, USA) enabled accurate and seamless adjustment of the per-pulse-energy (PPE) of the laser in the 1 µJ to 150 µJ range. PPEs were measured using a high-speed laser power meter (J-10MT-10KHZ, Coherent, USA). During OA measurements, a beam sampler (BSF10-A, Thorlabs, Newton, USA) redirected 1 % of each laser pulse to a fast photodiode (PD; DET10A, Thorlabs, USA) to reduce measurement errors induced by PPE fluctuations (approx. 5 % for the used wavelengths and PPEs). The beam size was adapted using an iris (SMD1D12SS, Thorlabs, USA) and was then focused into an optical fiber by a 100 mm focal distance lens (AC254-100-A-ML, Thorlabs, USA). A six-dimensional adjustable stage (K6XS, Thorlabs, USA) allows translation and rotation of the fiber input among three axes to adjust its position and orientation for high coupling efficiency (typically 80 % to 90 %). The fiber output was positioned within the central hole of an ultrasound (US) transducer, thus co-aligning the fiber's optical and transducer's acoustic axis (Estrada et al. 2014; Rebling et al. 2018). The small fiber core diameter of 105 µm combined with its low numerical aperture of 0.1 resulted in a 708 µm diameter spot at the working distance of 6 mm (FG105LVA, Thorlabs, USA). The custom-made polyvinylidene difluoride (PVDF) US transducer had a focal distance of 6 mm and 6 mm aperture diameter (Precision Acoustics, UK). Lateral resolution of approximately 60 µm was achieved with the effective transducer bandwidth of 30 MHz. Two stages mounted perpendicular to each other scanned the transducer over the sample reaching a velocity of up to 500 mm s^{-1} at 5 m s^{-2} acceleration (DDSM50/M, Thorlabs, USA)

while covering a field of view (FOV) of 50 mm x 50 mm. A dedicated pre-amplification system amplified the US signals by 8 dB directly at the transducer output followed by a low noise, broadband 24 dB amplifier (ZFL-500LN, Mini-Circuits, USA). The signal was then digitized by a data acquisition card (DAC; M4I.4420-X8, Spectrum Systementwicklung Microelectronic, Germany) which simultaneously acquired photodiode (PD) signals at a sampling frequency of 250 MHz. For each sampling position, 2400 samples were acquired corresponding to an effective sound propagation distance of 14 mm. A personal computer (PC) running Windows 10 and MATLAB 2018a (MathWorks, USA) collected the data (64 Gb RAM, Intel Core i7-6800K). Postprocessing was performed using Python 3 and MATLAB.

1.2 Fluorescence widefield microscope

A widefield camera (UI-2240-SE-M-GL, IDS, Germany) positioned concentrically over the Petri dish imaged the samples. Excitation light was delivered coaxially from below using a fiber coupled Tungsten light source (OSL2, Thorlabs, USA) providing 150 W unfiltered, broadband light. Two filter wheels (CFW6/M, Thorlabs, UK) were positioned in front of fiber output and camera objective, respectively. For R-GECO1, the excitation light was bandpass filtered around (559 ± 34) nm (MF559-34 - TXRED, Thorlabs, USA) and the emission light around (630 ± 69) nm (MF630-69 TXRED, Thorlabs, USA). The light source was used at full power (150 W) since illumination was provided from below through the Whatman filter paper. Exposure time was set to 2 s as a trade-off between acquiring sufficient signal in calcium ion (Ca^{2+})-unloaded state and avoiding saturation in Ca^{2+}-loaded state without having to change the exposure settings. A motorized stage (MTS50/M-Z8, Thorlabs, USA) moved the Petri dish in vertical direction to switch between loading position, Fluorescence (FL) imaging, and OA imaging. Acquired widefield images were corrected for camera distortion and light refraction at the water surface.

1.3 Scan procedure

Three-dimensional OA images were acquired in a mechanical overfly scan: a fast stage moved the transducer back and forth between scan window boundaries while the slow stage moved incrementally

after each line scan, resulting in an overall meander pattern. The slow stage carries a significantly higher mass (660 g) than the fast stage (30 g). Thus, scanning the full FOV containing 250 thousand sampled positions typically lasted 150 s using 5 m s^{-2} and 0.8 m s^{-2} acceleration for fast and slow stage respectively.

Triggering of the laser pulses and the subsequent digitization were based on the continuous position readings of the fast-moving stage. In this way, the sample was interrogated at an equally spaced grid of points regardless of stage acceleration and velocity. A microcontroller (Teensy 3.6, PJRC, USA) read out the x-stage quadrature encoder signal which provided a position accuracy of 500 nm. The laser and DAC were then triggered after a stage movement of 100 µm in both directions. For each scanning position, the data acquisition card (DAC) trigger was delayed by 106 µs to account for the laser delay. Due to position dependent triggering, no oversampling and excessive sample illumination occurred during acceleration and deceleration phases, further leading to optimization of the data size.

In order to accurately quantify performance of the protein variant expressed by a bacterial colony, we delivered a laser PPE of only 25 µJ (fluence of 6.54 mJ cm^{-2}, 10 nm pulse duration) through a multimode optical fiber (NA 0.1, 105 µm core diameter) to obtain a single-shot signal-to-noise ratio (SNR) higher than 20 dB. Since the scan step size was smaller than the illumination spot diameter (approx. 700 µm), each position was illuminated multiple times during a single scan resulting in an accumulated energy density of 62.5 mJ cm^{-2}.

1.4 Signal processing

Each recorded US signal was bandpass filtered between 0.5 MHz to 15 MHz, which reduced random noise and low frequency bias in the signals. To compensate for laser energy fluctuations, PPEs of shots were calculated based on the integrated PD signal and then used to normalize the measured US signals. The envelope of the filtered and corrected dataset was used to extract the OA signal intensity. For visualization, maximum intensity projections were calculated for the volumetric datasets. To reduce post-scan processing time, bandpass filtering, envelope extraction, PD correction, and maximum intensity projection calculation are performed during the scan. While the stages scan line i, post-

processing is simultaneously performed for line $i-1$. In this way, all the acquired data can be pre-processed and stored in memory during the scan.

1.5 Probing

Cell colonies were individually probed based on OA or FL images. To coregister coordinate systems of the two modalities, checkerboard phantoms were imaged. The FL image is then cropped, scaled, and rotated until it matches the OA image. For localizing the colonies, circular shapes were detected using the Hough transformation in either OA or FL images, resulting in a set of n center points (Yuen et al. 1990). A $n \times n$ cost matrix was calculated describing the time required to travel between distinct positions taking into account different achievable accelerations of the stages. The so called traveling salesman problem was solved using a genetic optimization algorithm (Beardwood, Halton, and Hammersley 1959; Ulder et al. 1991). After the approximate optimum trajectory was estimated, cells were probed individually. The optimized path can be used to probe the extracted positions over multiple timepoints or wavelengths as long as the Petri dish is kept in place.

1.6 Biological samples

Most genetically encoded calcium ion indicators (GECIs) were tailored towards a high relative change in their brightness upon Ca^{2+} delivery which is given by

$$\frac{\Delta F}{F_{min}} = \frac{\sigma_a \cdot \epsilon_a - \sigma_b \cdot \epsilon_b}{\sigma_b \cdot \epsilon_b} \tag{1}$$

where $\sigma_{a,b}$ quantum yield after / before binding to Ca^{2+}

$\epsilon_{a,b}$ extinction coefficient after / before binding to Ca^{2+}.

OA signal intensity is proportional to $(1-\sigma) \cdot \epsilon$ hence the maximum relative increase is defined via

$$\frac{\Delta OA}{OA_{min}} = \frac{(1-\sigma_a) \cdot \epsilon_a - (1-\sigma_b) \cdot \epsilon_b}{(1-\sigma_b) \cdot \epsilon_b}. \tag{2}$$

An increase in σ is thus related to a decrease in OA intensity. To select an appropriate starting point for screenings, several existing GECIs were compared (see Supplementary Material 2). R-GECO1 was identified as a promising variant and used to showcase probing functionality of the platform. The genetically encoded Ca^{2+} indicator R-GECO1 was *de novo* synthesized (GeneArt Strings, Thermo Fisher Scientific, Germany) and cloned into a modified variant of pRSETB (Invitrogen, USA) using SLiCe cloning (Zhang, Werling, and Edelmann 2012; Zhao et al. 2011). For imaging experiments purified plasmid was transformed into *E. coli* XL1 blue (Stratagene, USA) and plated on Lysogeny broth agar containing 100 µg mL^{-1} ampicillin (Carl Roth, Germany) to a density of approximately 500 to 800 colonies per Petri dish. Bacterial colonies were grown overnight at 37 °C to a size of 0.5 mm to 1 mm and subsequently incubated at 4 °C for 24 h to fully mature expressed sensors (Litzlbauer et al. 2015). Individual colonies rarely overlapped or fused which allowed us to distinguish between signals originating from different colonies. Ca^{2+} was delivered as previously described (Litzlbauer et al. 2015). Prior to imaging, the cells were transferred onto a Whatman filter paper which is subsequently placed within a new Petri dish. To keep colonies in place, the paper was covered with a thin Agar layer. For good acoustic coupling 30 mL of buffer were added to the Petri dish. After OA and FL imaging of the Ca^{2+} unbound state, Ca^{2+} was added to a concentration of 50 mmol dm^{-3}.

1.7 Optoacoustic and optical absorption spectrum of purified protein

Protein isolation and purification was performed as follows. His-tagged GECIs were recombinantly expressed at 37 °Covernight in 50 mL modified autoinduction medium in *E. coli* BL21 (DE3). Cells were harvested through centrifugation (5000 xg, 10 min, 4 °C) and resuspended in a 10 mL resuspension buffer (20 mmol dm^{-3} imidazole, Merck, Germany; 300 mmol dm^{-3} NaCl, Merck, Germany; 20 mmol dm^{-3} Na2HPO4, Merck, Germany; pH 7.8) supplemented with a protease inhibitor cocktail (4 mmol dm^{-3} PMSF, Sigma Aldrich, Germany; 20 µg mL^{-1} Pepstatin A, Sigma Aldrich, Germany; 4 µg mL^{-1} Leupeptin, Sigma Aldrich, Germany). Cells were lysed through sonication using a Bandelin Sonopuls (7 min, 80 % cycle, 80 % power). After lysis, the insoluble components were pelleted (18000 xg, 30 min, 4 °C). The supernatant was incubated with 150 µL of Ni-IDA agarose

beads (Jena Bioscience, Germany) overnight at 4 °C with light agitation. Beads were collected in gravity flow columns (Qiagen, Germany) and washed with 10 mL wash buffer (55 mmol dm^{-3} imidazole, 300 mmol dm^{-3} NaCl, 20 mmol dm^{-3} Na2HPO4, pH 7.8). Finally, proteins were eluted in 800 µL elution buffer (250 mmol dm^{-3} imidazole, 300 mmol dm^{-3} NaCl, 20 mmol dm^{-3} Na2HPO4, pH 7.8).

1 mmol dm^{-3} Ca^{2+} (stock solution 250 mmol dm^{-3}, Calcium chloride dihydrate, Honeywell, USA) was added to three batches containing 500 µL of the purified protein each to switch the protein into Ca^{2+}-bound state. Each batch was then divided into two 250 µL aliquots and 5 mmol dm^{-3} EDTA (stock solution 500 mmol dm^{-3}, Ethylenediaminetetraacetic acid, Sigma-Aldrich, Germany) was added to one of them to remove Ca^{2+} from the protein and revert it into the unbound state.

The OA spectrum was measured by injecting the aliquots in a polyethylene tubing (0.58 mm and 0.96 mm inner and outer diameters, respectively, Smiths Medical Inc. Minneapolis, USA) embedded in agar. The generated OA signals were collected with a custom-made 256-element spherical array (4 MHz central detection frequency, 100 % detection bandwidth, 40 mm radius and 90° angular aperture, Imasonic SaS, Voray, France) (Deán-Ben and Razansky 2013). Three-dimensional images were formed with a 3D back-projection algorithm that effectively averages the signals from the individual transducers, thus resulting in an enhanced SNR of the OA readings. Excitation was performed with a tunable optical parametric oscillator (OPO)-based laser (Innolas GmbH, Krailling, Germany). The laser beam was guided via a custom-made fiber bundle (CeramOptec GmbH, Bonn, Germany) to illuminate the tubing with optical fluence of 10 mJ cm^{-2}. The laser wavelength was tuned from 415 nm to 680 nm in 5 nm steps on a per-pulse basis. Acquisition was performed for 50 wavelength cycles and the images corresponding to each wavelength were averaged after reconstruction. No significant bleaching was observed by comparing the individual frames. The measured OA spectrum was normalized with the wavelength-dependent laser energy per pulse, which was estimated by injecting a black India ink solution (optical density 1, Higgins-Chartpak Inc. Leeds, USA) and comparing the OA readings with the ink spectrum measured with a spectrophotometer (Ocean Optics Inc. Largo, USA). The optical absorption spectrum of the purified protein was additionally measured in both Ca^{2+} loaded and unloaded state between 400 nm to 700 nm at 1 nm step size using a photospectrometer (Cary 100, Varian,

US).

1.8 Viability of bacteria after screening

To prove viability of bacterial colonies after imaging using pulsed laser irradiation, a plate containing R-GECO1 expressing *Escherichia coli* (*E.Coli*) colonies was further imaged at high PPE (50 µJ at 560 nm) before and after Ca^{2+} delivery following the described procedure. Afterwards, a colony providing good optoacoustic signal was picked, mechanically resuspended in buffer solution, and sprayed on a fresh agar plate. The plate was incubated overnight and checked for growth of bacterial colonies the following morning.

All code used for hardware control and evaluation of the datasets are available online: https://github.com/razanskylab/.

2 Comparison of existing sensor proteins for optoacoustic imaging

Table S1: Comparison of different red-shifted GECIs developed for FL monitoring of Ca^{2+} dynamics in the mammalian brain. λ_{ex} - excitation wavelength, σ - quantum yield, ϵ - extinction coefficient, FL - fluorescent brightness, OA_b - OA brightness, $\Delta FL/FL_{min}$ - relative fluorescence change upon Ca^{2+} delivery, $\Delta OA/OA_{min}$ - relative optoacoustic change upon Ca^{2+} delivery. [*] denotes $\frac{1}{\text{mM cm}}$. Related to Fig. 3.

Protein	λ_{ex} [nm]	σ_b [1]	ϵ_b [*]	FL_b [*]	OA_b [*]	σ_a [1]	ϵ_a [*]	FL_a [*]	OA_a [*]	$\frac{\Delta FL}{FL_{min}}$ [%]	$\frac{\Delta OA}{OA_{min}}$ [%]
K-GECO1(Shen et al. 2018)	568	0.12	19	2.28	17	0.45	61	27.45	34	1104	101
R-GECO1(Zhao et al. 2011)	577	0.06	15	0.90	14	0.20	51	10.20	41	1033	189
RCaMP1a(Akerboom et al. 2013)	577	0.12	35	4.18	31	0.45	57	25.52	31	511	2
RCaMP1c(Akerboom et al. 2013)	577	0.10	40	3.97	36	0.48	65	31.10	34	683	-6
RCaMP1d(Akerboom et al. 2013)	572	0.13	25	3.30	22	0.52	58	30.06	28	810	26
RCaMP1f(Akerboom et al. 2013)	572	0.11	17	1.91	15	0.48	59	28.27	31	1377	98
RCaMP1h(Akerboom et al. 2013)	571	0.14	19	2.62	16	0.51	65	33.20	32	1168	98
RCaMP1.07(Ohkura et al. 2012)	562	0.11	14	1.56	13	0.23	48	11.06	37	608	624
RCaMP2(Inoue et al. 2014)	563	0.11	14	1.56	13	0.23	48	11.06	37	608	193

3 Influence of delivery time onto calcium ion uptake dynamics

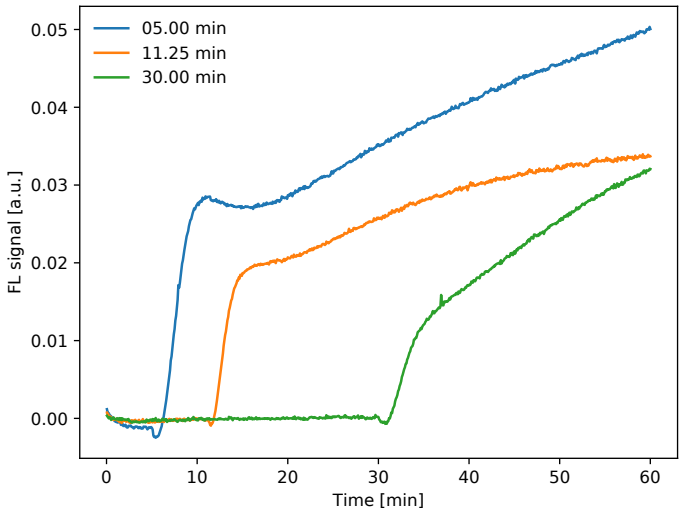

Figure S1: Influence of time between taking plates out of fridge and delivering Ca^{2+} on FL signal intensity: beside the time after Ca^{2+} delivery to the buffer medium, also the time after taking them from a cold fridge (7 °C) into a warm environment influences the dynamic behaviour of the protein response. If Ca^{2+} is delivered shortly after taking the colonies out of the fridge, the response occurs in general faster compared to long waiting times. All experiments within this paper were performed on plates just taken out of the fridge, related to Fig. 4C.

References

Shen, Yi et al. (Jan. 2018). "A genetically encoded Ca^{2+} indicator based on circularly permutated sea anemone red fluorescent protein eqFP578". In: *BMC Biology* 16.9. DOI: 10.1186/s12915-018-0480-0.

Estrada, Héctor, Jake Turner, Moritz Kneipp, and Daniel Razansky (Feb. 2014). "Real-time optoacoustic brain microscopy with hybrid optical and acoustic resolution". In: *Laser Physics Letters* 11.4, p. 045601. DOI: 10.1088/1612-2011/11/4/045601.

Rebling, Johannes, Héctor Estrada, Sven Gottschalk, Gali Sela, Michael Zwack, Georg Wissmeyer, Vasilis Ntziachristos, and Daniel Razansky (May 2018). "Dual-wavelength hybrid optoacoustic-ultrasound biomicroscopy for functional imaging of large-scale cerebral vascular networks". In: *Journal of Biophotonics* 11.9, e201800057. DOI: 10.1002/jbio.201800057.

Yuen, HK, J Princen, J Illingworth, and J Kittler (Feb. 1990). "Comparative study of Hough Transform methods for circle finding". In: *Image and Vision Computing* 8.1, pp. 71–77. DOI: 10.1016/0262-8856(90)90059-e.

Beardwood, Jillian, J. H. Halton, and J. M. Hammersley (Oct. 1959). "The shortest path through many points". In: *Mathematical Proceedings of the Cambridge Philosophical Society* 55.4, pp. 299–327. DOI: 10.1017/s0305004100034095.

Ulder, Nico L. J., Emile H. L. Aarts, Hans-Jürgen Bandelt, Peter J. M. van Laarhoven, and Erwin Pesch (1991). "Genetic local search algorithms for the traveling salesman problem". In: *Parallel Problem Solving from Nature*. Ed. by Hans-Paul Schwefel and Reinhard Männer. Berlin, Heidelberg: Springer Berlin Heidelberg, pp. 109–116. ISBN: 978-3-540-70652-6.

Zhang, Yongwei, Uwe Werling, and Winfried Edelmann (Jan. 2012). "SLiCE: a novel bacterial cell extract-based DNA cloning method". In: *Nucleic Acids Research* 40.8, e55–e55. DOI: 10.1093/nar/gkr1288.

Zhao, Y. et al. (Sept. 2011). "An Expanded Palette of Genetically Encoded Ca^{2+} Indicators". In: *Science* 333.6051, pp. 1888–1891. DOI: 10.1126/science.1208592.

Litzlbauer, Julia, Martina Schifferer, David Ng, Arne Fabritius, Thomas Thestrup, and Oliver Griesbeck (June 2015). "Large Scale Bacterial Colony Screening of Diversified FRET Biosensors". In: *PLOS ONE* 10.6. Ed. by Sabato D'Auria, e0119860. DOI: 10.1371/journal.pone.0119860.

Deán-Ben, X. Luís and Daniel Razansky (Nov. 2013). "Portable spherical array probe for volumetric real-time optoacoustic imaging at centimeter-scale depths". In: *Optics Express* 21.23, p. 28062. DOI: 10.1364/oe.21.028062.

Akerboom, Jasper et al. (Mar. 2013). "Genetically encoded calcium indicators for multi-color neural activity imaging and combination with optogenetics". In: *frontiers in Molecular Neuroscience* 6.2, pp. 1–29. DOI: 10.3389/fnmol.2013.00002.

Ohkura, Masamichi, Takuya Sasaki, Chiaki Kobayashi, Yuji Ikegaya, and Junichi Nakai (July 2012). "An Improved Genetically Encoded Red Fluorescent Ca^{2+} Indicator for Detecting Optically Evoked Action Potentials". In: *PLoS One* 7.7, pp. 1–7. DOI: 10.1371/journal.pone.0039933.

Inoue, Masatoshi et al. (Nov. 2014). "Rational design of a high-affinity, fast, red calcium indicator R-CaMP2". In: *Nature Methods* 12, pp. 64–70. DOI: 10.1038/nmeth.3185.